We are IntechOpen,
the world's leading publisher of
Open Access books
Built by scientists, for scientists

6,900
Open access books available

186,000
International authors and editors

200M
Downloads

Our authors are among the

154
Countries delivered to

TOP 1%
most cited scientists

12.2%
Contributors from top 500 universities

Interested in publishing with us?
Contact book.department@intechopen.com

Numbers displayed above are based on latest data collected.
For more information visit www.intechopen.com

Microfluidics for Time-Resolved Small-Angle X-Ray Scattering

Susanne Seibt and Timothy Ryan

Abstract

With the advent of new in situ structural characterisation techniques including X-ray scattering, there has been an increased interest in investigations of the reaction kinetics of nucleation and growth of nanoparticles as well as self-assembly processes. In this chapter, we discuss the applications of microfluidic devices specifically developed for the investigation of time resolved analysis of growth kinetics and structural evolution of nanoparticles and nanofibers. We focus on the design considerations required for spectrometry and SAXS analysis, the advantages of using a combination of SAXS and microfluidics for these measurements, and discuss in an applied fashion the use of these devices for time-resolved research.

Keywords: micro and nanoscale, systems design, lab-on-a-chip devices, SAXS, nanoparticles, time-resolved SAXS, microfluidics, hydrodynamic focusing

1. Introduction

Microfluidics is a multidisciplinary field dealing with the manipulation and behaviour of liquids and gases in dimensions below 1000 micron. The origin of microfluidics can be traced back to the 1970s, when miniaturisation became more and more developed. Applications in various fields, such as analytics, biology, chemistry, medicine and technology, became much more apparent with the development of *rapid prototyping*. Rapid prototyping describes a combination of photolithography, soft lithography and commercial printing, which makes the fast and efficient fabrication of custom designed microfluidic devices possible. Microfluidic devices for analysing aqueous samples were first introduced by Manz [1, 2], Harrison [3], Ramsey [4] and Mathies [5].

The most important benefit of microfluidic devices is their ability to perform quantitative and qualitative analysis with high sensitivity and resolution, while being a low cost method for fast, highly efficient analysis [6]. These factors make it especially useful for time resolved measurements, and coupling to small angle X-ray scattering (SAXS) measurements for the analysis of the average particle size and shape, and the evolution thereof under various *in situ* conditions. These approaches, in particular the coupling of microfluidics to SAXS, finds application in various areas, including biological materials, polymers, colloids, chemistry, nanocomposites, metals, minerals, food, pharmaceuticals and quality control [7].

Here we aim to detail background information important for the design of microfluidic devices for time resolved measurements, and the applications of these devices in time-resolved SAXS nanoparticle and self-assembly experiments.

1.1 Microfluidic principles

Fundamentally, the fluid dynamics in micro-dimensions are different from macroscopic systems. Fluid flows in these tiny systems are characterised by non-chaotic, smooth flow, where the fluid travels in parallel layers and the only interaction between those layers of flow is diffusion. By adapting reactions to microfluidic environments, the time axis of a reaction is converted into a distance axis along the outlet channel of the microfluidic device. This is key to enabling time-resolved studies *in situ* in a microfluidic channel.

The Navier–Stokes equation describes the motion of fluids mathematically, and is derived from Newton's second law of motion (F = ma), resulting in a set of two partial differential equations. For an incompressible Newtonian fluid, the Navier–Stokes equation is defined as:

$$\rho \left[\frac{\partial u}{\partial t} + (u \cdot \nabla) u \right] = \eta \nabla^2 u - \nabla p + F \tag{1}$$

where ρ is the density and η the viscosity of the fluid, p is the pressure, u the vector of the fluid flow, ∇ is the Nabla-Operator and F stands for any additional forces, that are directed at the fluid. The left side of the equation represents internal accelerations, and the right side represents the stress force per unit volume resulting from a pressure gradient and the viscosity of the fluid. In microfluidics, body forces are negligible, leading to a simplified, linear equation:

$$\eta \nabla^2 u = \nabla p \tag{2}$$

Treating the incompressible liquid as a continuum, the Navier–Stokes equation can be expressed as the continuity equation:

$$\nabla \cdot u = 0 \tag{3}$$

This means that the flux of liquid into a volume is the same as the flux out of a volume over a period of time. Additionally, the continuity equation is time-independent, restricting fluid flow in microfluidic channels to be symmetric in time [8].

To describe and compare phenomena on different scales, various dimensionless numbers for microfluidics were introduced. The most important is the Reynolds number (*Re*), showing the relation of inertial and viscous forces of a fluid. It is defined as:

$$Re \equiv \frac{inertial\ forces}{viscous\ forces} = \frac{|\rho\ (u \cdot \nabla)\ u|}{|\eta \nabla^2 u|} = \frac{\rho v}{\eta} d \tag{4}$$

where v is the flow velocity and d the characteristic length of the system, which in microfluidics is the diameter of the channel. The Reynolds number decreases with decreasing size of the system, reflecting the increased importance of viscous forces. The transition from turbulent to laminar flow is represented by *Re* being below 2040 ± 10.

The next most important dimensionless number is the Weber number (*We*), which describes the relation of the fluid surface tension to its internal forces, where γ is the surface tension of the fluid:

$$We \equiv \frac{\rho u^2 v}{\gamma} d \tag{5}$$

Microfluidic channel systems have generally a high surface-to-volume ratio, thus surface properties have significant effects on flow resistance and the velocity profile. To describe the interaction of a flowing liquid and a solid surface in microfluidic devices, Navier defined boundary conditions. The flow velocity tangential to the surface v_x is proportional to the shear stress at the surface and therefore given by:

$$v_x = \beta \frac{dv_x}{dy} \qquad (6)$$

β is the slip length, or Navier length, and is defined as the distance from a point inside the channel to the surface, where the velocity is zero. Where $\beta = 0$ is a "no-slip" condition, describing the interaction between fluids and walls [9].

Every biological process or chemical reaction is limited by the converging and mixing of the reactants. Mixing in fluidic systems can generally occur *via* two methods – diffusion or advection. On the macroscopic scale, mixing is achieved by "chaotic advection" or turbulence, while on the micron-scale it is driven by diffusion. Diffusion specifies the migration of particles along a concentration gradient, and thereby always takes place from an area of high concentration to an area of lower concentration. This flux is in proportion to the diffusion coefficient, D, given by Fick's first law of diffusion. Solving Fick's diffusion law for adequate boundary conditions, the diffusion coefficient can be described for spherical particles with radius r in low Re numbers by the Stokes-Einstein relation:

$$D = \frac{k_B T}{6\pi\eta r} \qquad (7)$$

with k_B as the Boltzmann constant, T as the temperature and η as the solvent viscosity. The relation between advection and diffusion for mass transport is described by the Péclet number (Pe) [8].

$$Pe \equiv \frac{advection}{diffusion} = \frac{vd}{D} \qquad (8)$$

For turbulent mixing, advection dominates the above equation, leading to high Pe numbers. In microfluidics, turbulent chaotic mixing is very difficult to achieve, because the Reynolds numbers are almost always very low. Thus, in microfluidic channels, advection is almost always very small, and diffusion dominates, resulting in Pe numbers that are low. As such mixer design in microfluidics devices seeks to optimise diffusion [10, 11]. Along microfluidic channels, diffusion becomes insignificant when compared to convection occurring far downstream at the outlet channel. Thus most mixing devices incorporate some method for laminating flows to reduce diffusion distances, and reduce mixing times. Most commonly, these mixers are simple Y- or T-shaped cross channels, and diffusive mixing in these types of mixers for kinetic experiments can be described by the following equations:

$$\frac{d_1}{d_2} = \frac{\eta_1}{\eta_2} \frac{Q_1}{Q_2} \qquad (9)$$

$$\frac{d_{MC}}{d_{SC_1} + d_{SC_2}} = \frac{\eta_{MC}}{\eta_{SC_1} + \eta_{SC_2}} \frac{Q_{MC}}{Q_{SC_1} + Q_{SC_2}} \qquad (10)$$

where d is the thickness of the relevant layer, η the viscosity and Q the volume flow. The following assumptions must be fulfilled for these equations to be true:

1. The microchannel inhibits steady and laminar flow.

2. The fluids are all Newtonian.

3. Density and viscosity of all fluids is the same in all channels and do not change during the experiment.

4. The channel geometry is rectangular and all channel parts have the same height.

Eq. (9) applies to Y-shaped channel geometries where layer 1 and 2 are the spaces of two introduced liquid streams in the inlet channels, which merge in the outlet channel. For T-shaped channels where two side channels (SC_1 and SC_2) hydrodynamically focus a main channel (MC) stream, Eq. (10) applies [12].

1.2 Principles of small-angle X-ray scattering

Small angle X-ray Scattering (SAXS) is an extremely versatile technique used for investigating particle size, shape and dynamics that can be applied to a wide range of scientific problems. It is amenable to a wide range of particles, from the very small, of around a few nanometres, to very large sized structures in the order of a micron. It can be used to study mixtures, and the evolution of shape in reaction mixtures, and is widely used in biophysics and structural biology to confirm structure, and investigate structures that are not amenable to other structure investigations. SAXS can be used across all states of matter, including solids, liquids, gases, semisolid sample such as gels, and plasma. We will focus here on solution scattering, as this is the most applicable for microfluidic applications.

We aim to provide a brief overview of SAXS for solution scattering and time resolved measurements, but highly recommend Feigin and Svergun, 1987 [13] for a more comprehensive in depth review of SAXS measurements. In general, a solution SAXS experiment is relatively simple (which is one of the great attractions for the technique). A sample, in an appropriate sample cell, is exposed to a focussed, collimated monochromatic X-ray beam, and at a distance away from the sample the intensity of scattered X-rays is recorded using a 2D X-ray detector (**Figure 1B**). The resulting image is termed a scattering pattern. Similarly, the scattering from a matched pure background solvent is collected, and then subtracted from the sample scattering pattern to provide a scattering pattern that arises purely from the sample particles. The variation of the scattered intensity with angle, where the measured angles are very small, is related to differences in electron density between the sample and solvent, and the interatomic distances inside the sample particle, and thus contains information on the size and shape of the particle.

Scattering in solution is generally considered isotropic, as most particle systems adopt random orientations in solution. This allows for analytical mathematical descriptions of the scattering profile on the basis of particle shape. Scattered intensity (I) is described as a function of momentum transfer, q, and in a simplified form can be given as:

$$I(q) = \frac{N}{V} V^2 (\rho 1 - \rho 2)^2 P(q) S(q) \tag{11}$$

Where N is the concentration of the particle in the solution, V is the volume of the particle, $\rho 1 - \rho 2$ is the contrast in electron density between the solvent and the particle, and q is defined as:

$$q = 4\pi \frac{sin\,\theta}{\lambda} \qquad (12)$$

Where θ is the angle from the incident X-ray beam to the point on the detector where the intensity is measured, and λ is the wavelength of the incident X-rays (see **Figure 1A**). The derivation of the dependence of scattered intensity on the volume, concentration and electron density contrast of a particle described in Eq. 12 is given in detail in [13], which we highly recommend for further reading. The form factor P (q) is typically a defined function, and varies depending on the physical parameters of the particle; for example a sphere with homogenous electron density has a different form factor function to that of a hollow sphere of the same size.

The structure factor component ($S(q)$) of Eq. (11) is a further analytical function that describes how the particles are arranged in the solution, e.g. forming large ordered structures with defined correlation lengths. Largely, samples are measured in a dilute condition, where the concentration of the particle is kept low enough to avoid these secondary interference effects, and thus $S(q)$ can be ignored. Where this effect cannot be avoided by reducing concentration, the use of hard sphere packing models or ionic charge–charge interaction models defining the effect as a function of q may be used to account for this effect, and provide information on changes in long range order in a sample.

Thus, for a sufficiently monodisperse sample, or a defined mixture of particles, it is possible to define an analytical model that provides volume, size and shape information. In polymer and colloid science, SAXS is used for many applications, including analysing the hierarchical nature of polymers in solution to assess clumping, local structure, overall morphology, and subunit arrangement, assessing the shape, size and dispersity of nanoparticles in solution, and investigating the dynamics, and evolution of particle size and shape under varying solution
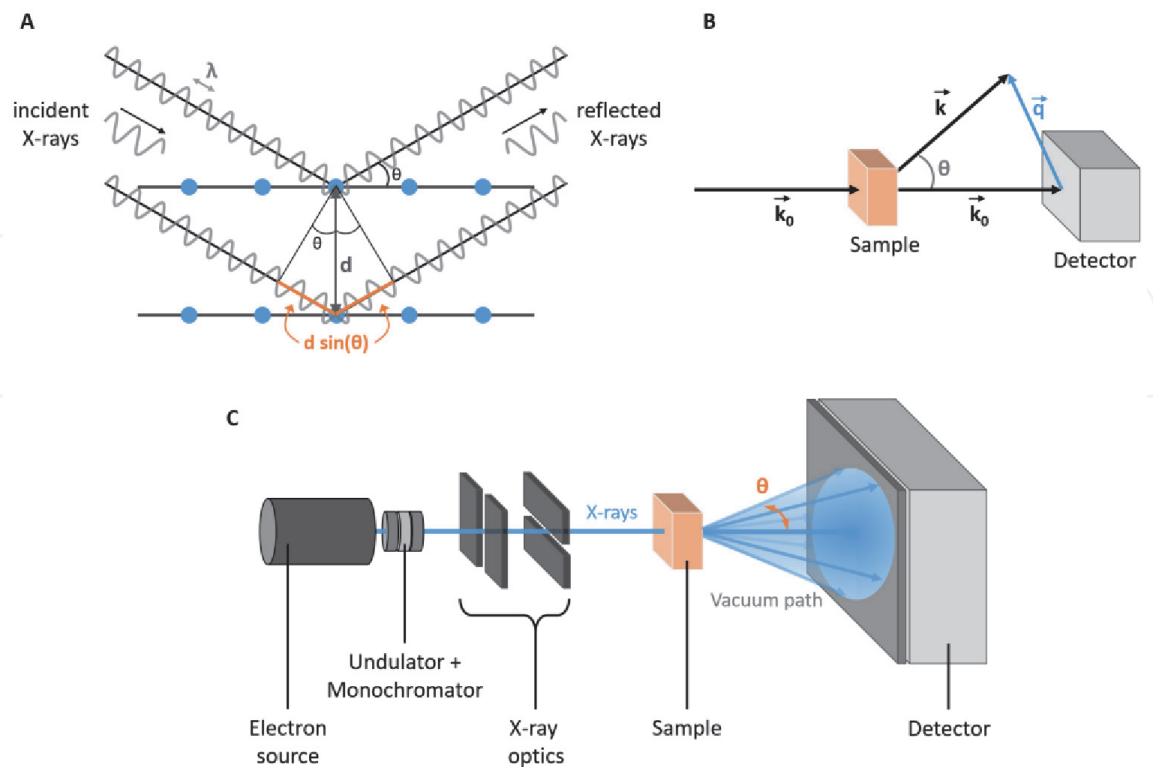

Figure 1.
(A) Schematic illustration of the Bragg equation with incident and reflected X-rays on two scattering planes, showing the lattice distance d, the half scattering angle θ, the wavelength λ and the path difference defined by Bragg's law. (B) Geometric construction of the scattering vector q from the incident wave vector k₀ and the scattered wave vector k with the half scattering angle θ. (C) Schematic setup of a small-angle X-ray scattering setup.

conditions and chemical reactions. SAXS is clearly a versatile technique that can provide useful information on systems that are well behaved, and can also be applied to samples that may not display ideal behaviour (for example aggregation prone nanoparticles, or time dependent mixtures of particles). However, the measurement does have some drawbacks. SAXS analyses are heavily reliant on complementary information. SAXS cannot provide information at an atomic resolution, so high resolution structural information is lacking, and needs to be obtained by alternative methods such as NMR, chemical crystallography, or electron microscopy. Further, SAXS does not provide information on changes in chemical environment so correlating the particle shape and size evolution with changes in the chemistry of a system requires the use of other techniques that are sensitive to the chemical environment. Additionally, for *in situ* experiments, SAXS on high intensity beamlines has the disadvantage that intense dose of radiation are required to obtain high quality data at short time frames. This can result in radiation damage in the sample that can significantly influence results.

1.3 Microfluidic devices and X-rays

In SAXS analyses, there are a range of disadvantages that the current sample environments struggle to address. First and foremost is that in most solution SAXS measurements there needs to be a high concentration of particles in the solution to achieve a scattering signal with high enough signal to noise to be of use in further analysis. For the most part, this is not a significant issue as most samples are generally amenable to reasonably high concentrations. However, in a number of cases, the amount of sample can prohibit the use of standard sample environments, and limits the use of SAXS to samples that are not in limited quantities, or expensive to produce. Further, for a continuous flow mixing device, where many exposures are required at each time point, the sample consumption can reach many millilitres; again this may be prohibitive for a majority of samples. Additionally it can be difficult to apply high throughput methodologies to systems where flow, volume and data quality constraints limit the number of measurements that can physically be conducted in a period of time.

The limitations of the current sample environments can be significantly mitigated by the use of custom microfluidic devices. The very low internal volumes mean that sample consumption is reduced, and the time that a volume of sample can be measured over under flow is increased, leading to a general improvement in measurement statistics. The lower spatial footprint, and lower sample consumption rates, means that a large number of measurements can be conducted in a very short period of time in parallel; increasing throughput for screening measurements. The lower volumes, and thus much more efficient mixing allows for much lower deadtimes then would otherwise be possible, and with the increasing access to microbeam SAXS measurements, the time resolution of the mixing experiments are greatly improved over conventional approaches. Further, the ease of design and modification of devices means that bespoke devices for specific applications can be achieved rapidly. Given that microfluidic devices can address many of the limitations of conventional SAXS sample environments, we believe that there will be increasing uptake and incorporation of these devices into SAXS measurements.

2. Microfluidics for time-resolved studies

2.1 Device design

To successfully investigate time-resolved reactions in microfluidic devices, the channel design has to be carefully adapted to the requirements of each application.

All experiments require planning and consideration of the simultaneous use of analysis, mixing and cleaning equipment due to the generally small dimensions of microfluidic devices. In the past decades, a very diverse range of microfluidic reactor devices have been designed for time-resolved studies of reactions. Designs such as continuous-flow, stopped-flow, droplet-based and digital microfluidics have been developed and applied to produce materials with sizes ranging from nanometres to almost millimetres. In this chapter, we are focusing on continuous and stopped flow devices, in particular on hydrodynamic focusing techniques. In comparison to droplet-based techniques, hydrodynamic focusing is a straight-forward approach to implement, due to its pure hydrodynamic principles. It only includes surface tension effects at the liquid–liquid interface in the outlet channel of the microfluidic device without the need of consideration of surface tension effects at liquid–gas interfaces. These devices offer stability at high flowrates, allow high-throughput applications and enable highly controllable operational conditions, as the flow behaviour is the only influential parameter that needs to be considered for time-resolved studies.

2.1.1 Flow field considerations

An understanding of flow fields at the microscale is required to understand the function of hydrodynamic focusing and device design considerations. No turbulent mixing occurs inside a microfluidic channel, as typically *Re* numbers below 100 are achieved, thus liquids can only mix by diffusion. This has the advantage of allowing predictions of the exact movement of particles by calculation, as no chaotic (turbulent) mixing needs to be considered.

For microfluidic channels, assuming no-slip conditions in combination with pressure driven flow, Poiseuille flow with a parabolic shaped flow profile arises. Here, the highest velocity is in the middle of the channel, which decreases parabolically towards the walls until it reaches zero. For cylindrical shaped channel geometries with coordinate length x, radius r and azimuthal angle Φ, the velocity field can be derived as:

$$\nu_x(r, \phi) = -\frac{\Delta p}{4\eta L}\left(a^2 - r^2\right) \qquad (13)$$

With pressure p and viscosity η over the channel length L and channel radius a. The hydraulic resistance R results then as:

$$R = \frac{8\eta L}{\pi a^4} \qquad (14)$$

For rectangular shaped channels with height h, width w and small aspect ratio $(w > h)$ the velocity field over the coordinates x, y, z is:

$$\nu_x = \frac{4h^2 \Delta p}{\pi^3 \eta L} \sum_{n,\,odd}^{\infty} \frac{1}{n^3}\left[1 - \frac{cosh\left(n\pi\frac{y}{h}\right)}{cosh\left(n\pi\frac{w}{2h}\right)}\right] sin\left(n\pi\frac{z}{h}\right) \qquad (15)$$

and the hydraulic resistance R is then [14]:

$$R = \frac{12\eta L}{wh^3}\left[1 - \frac{h}{w}\left(\frac{192}{\pi^5}\sum_{n=1,\,3,\,5}^{\infty}\frac{1}{n^5} tanh\left(\frac{n\pi w}{2h}\right)\right)\right]^{-1} \qquad (16)$$

This understanding of this pressure-driven, steady-state flow in microfluidic channels is the basis of liquid handling in lab-on-chip systems. Especially in microfluidics, the channel cross-sections can be of various shapes, depending on the application and fabrication method. Eqs. (13) to (16) describe the velocity field and hydraulic resistance for spherical and rectangular cross-sections, which are the most common geometries used for the devices described in this chapter. The derivation of those values is exceedingly more complicated for arbitrary channel cross-section shapes.

2.1.2 Continuous flow vs. stopped flow

The first design consideration is how the device will enable time-resolved measurement of phenomenon. This can be achieved in two different ways. The first, and conceptually simplest method, is a static experiment, where a sample is firstly mixed and then introduced into a monitoring chamber and measured repeatedly at defined time periods. The most common apparatus for this style of measurement this is a *stopped flow* device, where mixing is achieved rapidly, and then flow is stopped as soon as the homogenously mixed sample fills the monitoring chamber. The measurement is triggered as soon as the flow is stopped, and generally continues as rapidly as possible until the reaction reaches completion. The second method is to use a continuous flow system, where the mixed sample is introduced into a flow-through system, and temporal measurements are achieved by varying the distance between the mixing point and the sampling point.

Both styles of devices have advantages and disadvantages, and the choice depends strongly on several experimental considerations, including the time domain of the reaction, mixing efficiency, sample volume constraints, and sample chemistry constraints (e.g. resistance to photobleaching, or radiation damage). Stopped flow measurements are favoured when there is a small volume of sample that is resistant to measurement induced damage (for example a flurophore that is resistant to photobleaching), where the reaction is not extremely fast, and where the experimental measurements are not slow. In stopped flow measurements the initial point in the measurement is always some degree of time post the start of the reaction (given the time it takes to fill the sample cell, stop the flow and take the first measurement), and the temporal resolution of the measurement is given by the speed at which the measurement can be taken. However, agglomeration of the reacting sample on the channel walls can influence the quality of measurements and, due to the ongoing reaction, leads to only a small window that can be detected before the experiment needs to be repeated. Alternatively, continuous flow measurements favour samples that are sensitive to the measurement, are very rapid, and require temporal resolution finer then the measurement speed of the instrument. Continuous flow measurements allow for measurement very close to the point of mixing, temporal resolution is given by the spatial resolution of the measurement, and the time taken to travel to the point of measurement. Further, the deadtime and temporal resolution is heavily influenced by flowrate, allowing for fine control across many temporal regions. As a result, the observation of the reaction can be precisely controlled. It needs to be considered that continuous flow measurements need more sample volume in comparison to stopped flow methods, to provide a constant flow profile.

2.1.3 Hydrodynamic focusing

The basis of hydrodynamic focusing lies in a central solution that flows with a lower flowrate within an outer sheath fluid with a higher flowrate. This enables the

compression, or focusing, of the central flow, and decreases the mixing times significantly by reducing the diffusion length. There are two main categories for microfluidic devices with hydrodynamic focusing: coaxial tube and planar on-chip devices. The design can be defined depending on the use, with adapted geometries for fast mixing (**Figure 2A**), gradients (**Figure 2B**), specific nanoparticle growth reactions or self-assembly processes (**Figure 2C**) [15].

The simplest type of coaxial tube reactors is a device consisting of two concentric capillaries (**Figure 2D**), which are connected to a channel where a central flow is injected through the inner capillary, with sheath flow injected from the outer layer. Coaxial tube microreactors find various applications, but are typically used as the interface for droplet-based reactors, as the transition from flow to droplet generation, dripping and jetting is defined by the flowrate of the outer sheath flow. However, this approach is of limited utility in time resolved mixing applications, as it only offers limited mixing geometries. Further limitations abound in the fabrication process for coaxial designs, which requires multiple steps and precise alignment and assembly of the parts [15].

On-chip hydrodynamic focusing devices can be differentiated in two-dimensional (2D) and three-dimensional (3D) devices. In two-dimensional hydrodynamic focusing devices, the central flow is focused in the horizontal plane. The simplest geometry for a 2D device is a Y- or T-shaped mixer (**Figure 2E**), where the cross-sectional diffusion is broadened at the channel walls in comparison to the centre. However, this design is highly limited regarding flow stability and focusing and susceptible to variation in these parameters in operation. To avoid this, cross-
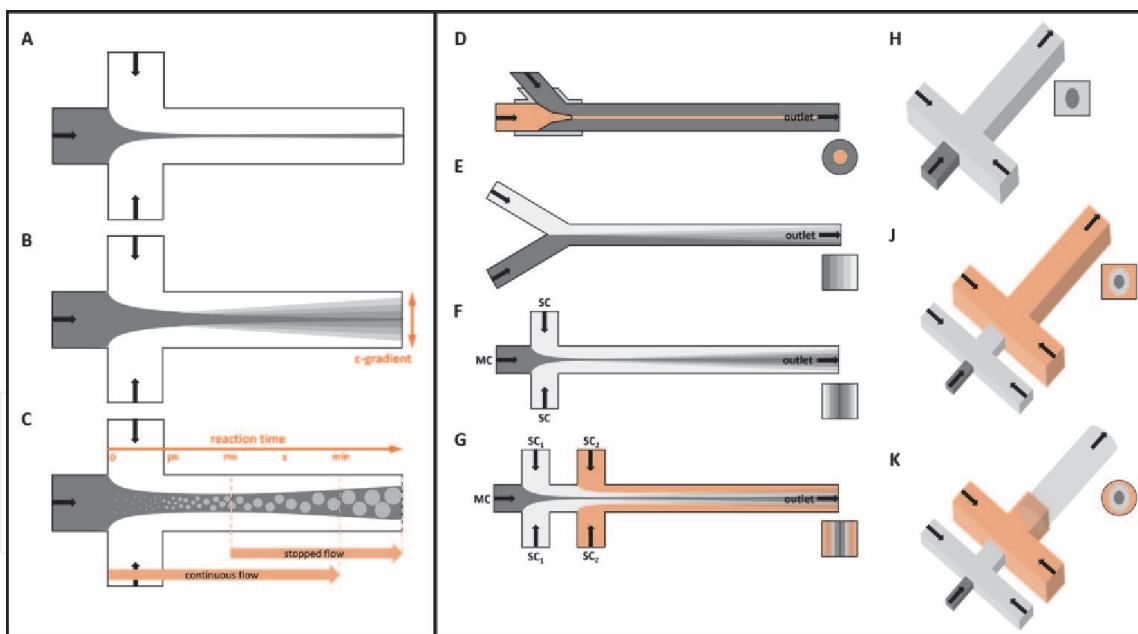

Figure 2.
Left: Scheme of microfluidic features for kinetic investigations in flow in a cross shaped mixer. (A) Hydrodynamically focused Centre stream for fast mixing experiments. (B) Mapping of concentration gradient across and along the channel through interdiffusion of different liquids from main and side channels. (C) Nucleation and growth of nanoparticles or self-assembly processes of nanomaterials as a function of time along the outlet channel. Schematic comparison of the provided time scales in continuous and stopped flow microfluidic devices. Right: Schematic illustration of microfluidic devices with various channel cross designs with the corresponding cross-sections through the outlet channel. (D) Coaxial tube reactor with two concentric channels/capillaries. (E) Y-shaped design, where mixing is solely based on diffusion. (F) Cross-shaped geometry at the inlets for hydrodynamic focusing. (G) Two-cross-section geometry, also known as double-focus device, where three different solutions can be introduced into the channels. Solutions introduced into the first side-channel (SC$_1$) act as an inert buffer between reactants in main channel (MC) and second side-channel (SC$_2$). (H) and (J) multilayer designs of the geometries from (F) and (G), respectively, avoiding contact between the central stream and channel walls. (K) Hybrid device consisting of multilayer focusing device (J) and an inserted glass capillary as outlet channel.

shaped geometries can be employed, where the central flow is focused from both incoming side channels (**Figure 2F**). This provides good control over the thickness of the central stream. Furthermore, it allows a well-defined sample composition that can be adapted by variation of the volume flow in each inlet individually. To adapt the device design to multi-step synthesis, several side channels can be added to introduce additional reactants (**Figure 2G**). Thus planar on-chip hydrodynamic focusing is more highly favoured for flexible mixing devices, and is used much more often in general microfluidic designs.

However, there are further considerations that need to be taken into account, particularly for chemical reactions or self-assembly processes. In coaxial and 2D channel geometries the interface of reacting solutions is in contact with the channel walls, and particles or macromolecules can stick and agglomerate on the channel surface and disturb the laminar flow conditions. Furthermore, this accumulation interferes with analytical investigations and, in the worst case, can cause complete blockage of the channel.

To avoid channel contact, three-dimensional channel geometries can be used. 3D hydrodynamic focusing requires both horizontal and vertical focusing of the central reactant stream, leading to a complete enclosure with liquid from all sides (**Figure 2H** and **J**). The device design can be optimised to reach homogeneous mixing without integrating specific mixing regions before the measurement part of the microfluidic chip. Additionally, these devices are simple to fabricate and have easily adjustable designs. The most common design to achieve 3D hydrodynamic focusing is through multi-layer on-chip devices, which require precise alignment as part of the fabrication process. Alternate methods are single layer devices or novel fluid manipulation technologies like "microfluidic drifting", which introduces lateral drifts or counter-rotating vortex forces to achieve vertical and horizontal flow focusing. These alternatives require less alignment in manufacturing and are thus much more user friendly in regards to fabrication.

All previously described device geometries can be used to produce droplets, liquid jets and sprays under the right flow conditions, including ultra-high flowrates. These devices are not limited to constrained flows inside channels, and for time-dependent studies the use of free liquid jets is preferred. Measurements of free jets have significant advantages in many optical measurements, as there is little to no background signal from surrounding material. When employing free jet devices, the parabolic flow profile from laminar flow within channels turns into a plug flow profile after passing the nozzle outlet. The liquid–solid interface of the no-slip condition resulting in parabolic flow is replaced by the liquid–gas interface in air, which has lower friction with the fluid and can be accelerated in flow direction. Free jets, however, are also quite difficult to work with, and despite the advantages in background have not found widespread use in the field.

2.2 Fabrication

2.2.1 Fabrication techniques

Many different technologies exist for the production of microfluidic devices. In general, fabrication of microfluidic devices in hard materials is often very time-consuming and cost-intensive, thus polymers are generally preferred, particularly when cost and ease of fabrication are considerations in the design process. In most cases, designs are started in silicon, with a Computer-Aided Design (CAD) model of the device. The device is then fabricated using any of a number of different technologies following a process of rapid prototyping. We focus here on some of the more common approaches.

Lithography. One of the most powerful methods in microfabrication is lithography. It can be differentiated by the type of radiation used, e.g. photolithography, electron-beam lithography, or X-ray lithography. With these different lithography methods, structures with sizes between 0.2 and 500 μm in hard materials like glass, or between 0.5 and 500 μm in soft materials like polymers, can be achieved. In the most common form of lithographic fabrication, a UV blocking mask is generated from the CAD model, and adhered to a silicon wafer. The master model for fabrication is then generated by photolithography, where the masked wafer is coated in a photosensitive epoxy monomer solution, and UV-cured. In general these silicon masters are then used to generate working devices via soft lithographic replication. The most common approach is to use the master chip as a mould, and poly (dimethylsiloxane) (PDMS) to form an imprinted device, which can be bonded to a glass-slide or a second PDMS part to form the final microfluidic device [16–18]. The replicated structure can be a positive or negative of the initial design, depending on which part of the structure was UV-cured on the silicon master.

Hot embossing and micromoulding. Hot embossing is a micromoulding technique that uses thermoplastic polymers to imprint structures at elevated temperatures. It usually uses high-temperature polymers, e.g. PMMA, PC, PI, PE, PVC or PEEK, which are heated above their glass transition temperature (T_g) before being pressed into a mould with high pressure. The moulds have to withstand the applied pressure and high temperatures, and are often made of metal or silicon, fabricated via etching, lithography in combination with electroforming and moulding or CNC (Computerised Numerical Control)-machining. The accuracy of hot embossing is in the order of tens of nanometres, making it possible to obtain high aspect ratios of structure, while being a low cost and easy procedure. It is often used with a defined and tested device design as high throughput method with a very short fabrication time [19, 20].

3D printing. Within the last decade, 3D printing technologies have advanced to astonishing precision, in size-regimes down to the micrometre scale. Additive manufacturing technologies like fused deposition modelling (FDM), stereolithography (SLA) or selective laser sintering (SLS), have been developed for various materials like polymers, resins, ceramics or metals. It is possible with these techniques to produce a complete microfluidic device in one step. The device material and process can thereby be selected with regard to required mechanical and chemical properties of the device. A channel size resolution of few hundred micrometres can be achieved, making this approach preferred for devices with wider channels [21, 22].

2.2.2 Device materials

Based on the desired purpose of the microfluidic chip, device materials must fulfil specific criteria. The most important requirements which will be addressed in this chapter are solvent stability, ease of fabrication, and optical and X-ray transparency.

Solvent stability. Microfluidics deals with the manipulation of liquids, which means that the device material has to be resistant and inert to the solvent. This becomes especially relevant when using organic solvents, as they often cause swelling or dissolution of standard polymeric device materials. Swelling leads to deformation, which can cause channel closure. A number of device materials have been tested with regard to resistance to some common solvents for nanoparticle synthesis and self-assembly processes (**Table 1**). It is clear from these results that careful selection of polymer is necessary for long term stability.

Ease of fabrication. While the solvent is important, it is also essential to consider the difficulty of working with the various polymers, and the end

Polymer Solvent	PDMS	NOA 81	THV815 GZ	THV610 AZ	THV500 GZ	THV221	ET 6235	HTE-1705Z	PS	PMMA	TOPAS 8007/6013	Bendlay	SIFEL	SU8 50
THF	x	x	x	o	o	x	o	(x)	x	x	x	x	o	o
Toluene	x	(x)	x	o	o	o	o	o	x	o	x	x	o	o
Chloroform	x	x	x	o	o	o	o	o	x	x	x	x	o	o
Dioxane	(x)	x	x	o	o	o	o	o	x	x	o	x	o	o
Acetone	o	o	x	x	o	x	o	o	x	x	o	x	o	—
Octadecene	o	o	x	o	o	o	o	o	o	o	x	o	—	—

x: dissolution or swelling of the material, o: no change observed, −: not tested. Results in () showed insignificant swelling, the device could be continued to be used [23].

Table 1.
Stability test of various polymers and the corresponding solvents.

characteristics of the device. For example, NOA 81 is a turbid, commercially available, UV curable polymer mixture from Norland Optical Adhesive, which is relatively easy to work with. However, devices made from NOA 81 are thin and relatively flexible, even after sealing top and bottom half, so it should be avoided if stiff or thick devices are required. In comparison, SIFEL (SIFEL2610) is a fluorinated polymer distributed by Shin-Etsu that is liquid at room temperature and hardens at higher temperature, and is stable against all tested organic solvents. The device fabrication however, is time consuming, requiring the additional step of sputtering the silicon wafer with an inert chemical layer to allow release of the SIFEL device from the mould.

Materials can also dictate the method of fabrication, for example THVs (fluorothermoplastics of blended tetrafluoro ethylene, hexafluoro propylene and vinylidene) must be fabricated by hot embossing. Glass or hard material devices are made with difficult fabrication techniques, like etching. In many cases prototypes are made with cheap, easy to fabricate materials, with the more difficult fabrication only for the final working devices where needed.

Optical and X-ray transparency. The most commonly used method for alignment of device parts and analysis of ongoing reactions is optical microscopy. Hence, the optical properties, e.g. transparency, of the microfluidic devices should be considered. Further, the final measurement modality must be considered in material selection. For example, if three-dimensional confocal microscopic investigations of the whole channel volume are required, the selected device material should provide a low absorption behaviour in the range of the sample-specific selected laser wavelength, and low fluorescence background. Or as the focus of this chapter is SAXS, the material of the device should have high X-ray transmission, and low scattering in the q-range of interest. The material should also be able to withstand the X-ray radiation, which is present on high flux SAXS beamlines. In our experience, the lowest background scattering for higher q measurements above 0.05 Å^{-1} were achieved with glass, NOA81, PDMS and Kapton. Other polymers such as THV and TOPAS showed diffraction and correlation peaks in the high q region >0.1 Å^{-1}, that interfere with background subtraction, and worsen signal to noise. For measurements at low scattering angles with q values under 0.05 Å^{-1}, glass, PMMA, PS, NOA81 and TOPAS display flat scattering curves. All other tested materials at this q-range showed significant scattering signals from the device [23]. Furthermore, although showing a low scattering background at high scattering vectors, PDMS was extremely sensitive to radiation, deforming the channel and showing an increasing and changing scattering profile with exposure. This material is typically unsuitable for SAXS measurements.

Hybrid microfluidic devices can marry the best characteristics of materials, to achieve a successful device. For example, the complex mixing cross section can be made from easy to handle materials, e.g. PDMS, and a robust X-ray transparent, low background scattering material inserted as an outlet channel after the last cross-section, e.g. a glass capillary (**Figure 2K**). These devices have the advantage of high optical and X-ray transparency in the measurement region, while allowing adjustment to the mixing cross design in the polymer part [23, 24].

2.3 Practical considerations for device handling

2.3.1 Fluid handling

A key practical consideration for the use of microfluidics is the method for introducing fluid into the device. For the most part, each interface channel should have its own fluid handling system, which should be capable of smooth, pulse free

flow, with no bubbles or leaks, and should have similar chemical compatibility to that of the microfluidic device [25]. We favour modular syringe pump systems, which have the ability to adapt the amount of dosing units to the number of channels. Other options include flow regulated gear pumps, positive air pressure systems or even on-chip fluid reservoirs. In any case, fluid flows should be accurately calibrated immediately prior to use, to ensure the correct dosage, flowrates and thereby the correct flow profile. A further consideration in fluid handling is minimising dead volumes (in particular by using appropriate fluidic connections and minimising tubing lengths), to prevent wastage of sample. Further, it is ideal, particularly for time resolved SAXS experiments where access to the system is restricted, if the fluid handling system can be controlled and triggered remotely, as this allows for accurate initiation of the reaction and data acquisition. The usability of all devices should be tested before each experiment to avoid leakage and proper function of the channels, especially with regard to flow focusing. Tubing and device failure are common frustrations in obtaining good data.

2.3.2 Temperature control

In general, homogeneous temperature control of the reaction solution has to be achieved. It is possible to submerge the whole microfluidic device and tubing in a water / oil bath. However, for *in situ* investigation, there needs to be unimpeded access to the channel, and this approach is thus not viable. In this case, custom designed heating elements, e.g. heated enclosures, are employed to regulate temperature. Temperature control is only limited by the geometric constraints of the measurement, and the heat transmission of the device material. For example, we have implemented copper heating tubes for surrounding the glass capillary of hybrid microfluidic chips, incorporating a window for the X-ray beam that provided excellent thermal control of the measurement [26, 27]. A key to good thermal stability is to also incorporate heating elements for the fluidics systems, to keep the reaction solutions at appropriate temperatures and ease the thermal load on heating elements in the device.

3. Microfluidics and SAXS

3.1 Incorporating microfluidic experiments into SAXS

After the microfluidic devices are designed, fabricated, tested and fluid control is established, final considerations involve the implementation of the complete setup in an X-ray beam, either in a SAXS lab instrument or at a synchrotron beamline. Depending on SAXS instrument design a number of adjustments and considerations are required to achieve good integration for the measurement. As every synchrotron has slightly different parameters and sample environments, it is recommended to contact the beamline staff if considering a microfluidic-based time-resolved SAXS experiment for specific advice.

3.1.1 Device modifications

SAXS measurements are dependent on the volume and composition of all objects in the X-ray beam. Consideration should therefore be given to not only the material's resistance to radiation damage, but also the relative volumes of device material and sample that are going to be presented over the measurement channel. For example, 2–3 mm of any device-polymer either side of a sample channel of 50

micron means that the scattering from the sample in the channel will be entirely masked by the scattering of the polymer device, even if the polymer scattering is low. Further, the more material that is in the beam pathlength the more attenuation of the X-ray beam will occur. This means that less photons will hit the sample, get scattered, and escape the device to be detected. Calculations based on composition and thickness of the material should be done in advance to determine the expected transmission of the device. In many cases, this requires a redesign of the device itself to thin down the supporting material around the channels, incorporate X-ray transparent windows, or change the device material.

3.1.2 Device mounting in beamline/SAXS instrument

It should be expected that the device will be required to be perpendicular to the beam. Further consideration should also be given to the orientation of the channels, with respect to the beam dimensions. Generally, it is optimal to orient the channels so that as much of the beam is going through the channel as possible, and as little as possible is hitting the device body. This minimises background, and optimises the signal that can be achieved. In the best case scenario, the beamline will have the capability to generate micro beams of a few micron in any dimension. This allows for optimal exposure for the sample, and greatly increased time resolution in time-resolved samples.

It is best if the device has a chip-holder to mount the device in, which in most cases is specific to the setup and design. This holder must allow for any necessary connections of inlet and outlet tubing while holding the microfluidic device steady and without tension on any connections to pumps or vials. Ideally, this holder would be placed on a motor-controlled, adjustable stage to facilitate precise alignment in the X-ray beam and movement of the device to scan along outlet channels for different points in time of reaction kinetics.

In many cases, beamlines and lab instruments will maintain a vacuum along the complete X-ray flight path, and may include a vacuum sample environment. As X-rays interact with all matter, it is a requirement that there not be air in the majority of the SAXS instrument. Vacuum sample environments take this further by removing all air in the system to reduce and minimise background scattering. If a vacuum sample environment is in use, the microfluidic device must be designed to withstand the vacuum levels, and to minimise outgassing and other deleterious effects.

3.2 Nanoparticle nucleation and growth

A fundamental principle in nature and technology is self-assembly – the formation of ordered structures of components of a system out of chaotic arrangements without external forces. These processes can be induced by a multitude of parameters, e.g. change of solvent, pH, temperature, pressure or by introduction of additional reactants. SAXS, being sensitive to length scales of 1–100 nm is an ideal technique for studying nanoparticle size and structure from nucleation to the final particle. *In situ* SAXS measurements of nanoparticle synthesis is typically used to monitor the kinetics of this process [7], and increasingly incorporates microfluidics.

Metal nanocrystals. Metal nanoparticle syntheses is particularly amenable to SAXS analysis, as their high electron density contrast allows measurements in dilute suspensions even at the very early stages of particle nucleation. This has been employed for investigating silver (Ag) and gold (Au) nanoparticle formation and structure [28–31]. The first steps towards microfluidic setups were stopped flow measurements, for example the kinetics of gold nanoparticle formation, and the

concurrent evolution of the optical properties of the particle at room and high temperature was very successfully investigated at millisecond resolution with this method by Abécassis et al. [32, 33] and Chen et al. [26]. Further development by Polte et al. provided *in situ* studies on the nucleation and growth of Au and Ag nanoparticles in stopped and continuous flow microfluidic devices [34, 35] Free liquid jets coupled to microfluidic mixers have aided in reducing background and improving signal to noise of SAXS measurements [36].

When combining microfluidic setups and X-ray scattering for nanoparticle investigation, not only the reaction kinetics of nucleation and growth processes can be measured, but also agglomeration kinetics and structures. For example, Gerstner et al. combined a static microfluidic mixing device with in line absorption and SAXS measurements to study the rapid superlattice formation of alkylthiol-coated Au nanoparticles at different temperatures, which showed a differentiation between long- and short-range self-assembly effects of temperature on a time scale down to 3 seconds [37]. A further example is the time-resolved analysis of polystyrene (PS)-coated Au nanoparticles by Merkens et al. in a Kapton-based 3D hydrodynamic focusing microfluidic chip, that revealed the subsecond kinetics of structural transitions involved in solvent induced collapse [38].

Semiconductor nanocrystals. Inorganic semiconductor nanoparticles, also called quantum dots (QDs), have received much attention due to their bright and size-tunable photoluminescence, which is commonly used as a key measurement property during synthesis [39]. During a synthesis of QDs, inorganic particles undergo a process of nucleation, growth and agglomeration, followed by dispersion into a buffer solution to quench the reaction. In order to synthesise homogeneous particles it is important to induce rapid nucleation and control the growth rate. Microfluidic devices with hydrodynamic focusing have been extremely useful in achieving this controlled synthesis process [15]. We have used 3D hydrodynamic focussing device for the synthesis of CdS nanoparticles, both studying the reaction by confocal laser scanning microscopy (CLSM) and SAXS. The CLSM measurements, using a full-PDMS device, showed the increase and shift of photoluminescence related to the nucleation and growth of CdS nanoparticles along the outlet channels. Hybrid microfluidic chips, consisting of the mixing cross section in PDMS and an inserted glass capillary as outlet channel (**Figure 3D-F** D-F), were developed for *in situ* SAXS measurements with low scattering background [24]. Employing a stopped flow setup, the nucleation and growth of ZnO nanoparticles was characterised at the timescale of seconds [27]. Further work elucidated the kinetics of the process at the microsecond timescale, using a free-jet device with a microfluidic T-mixer setup with a nozzle outlet to perform synchrotron SAXS measurements of the reaction in air (in the free jet). These setup enabled the investigation of QD synthesis with and without stabilising agents [42], highlighting the use of microfluidics and SAXS in the development of straightforward processes for nanoparticle synthesis.

3.3 Macromolecular self-assembly

Structural evolutions of pure and mixtures of surfactants that are often used in nanoparticle synthesis reactions, can also be investigated by a combination of microfluidic platforms and SAXS. Fürst et al. used a simple, T-shaped microfluidic chip to measure the structural assembly of tetradecyldimethylamine oxide (TDMAO) and lithium perfluorooctanoate (LPFO) in combination with synchrotron SAXS. This revealed the kinetic fusion mechanism of the cylindrical TDMAO and spherical LPFO micelles to disk-like micelles as a diffusion limited process, resulting in lamellar correlations at final stages [23].

Amphiphilic diblock copolymers show fast self-assembly processes at a timescale of seconds. These can be followed *in situ* with specially designed equipment by synchrotron-based SAXS, as shown by Stegelmeier et al. for PS-P4VP block copolymers by rapid removal of solvent [43]. An elegant way to study these fast self-assembly processes *in situ* in solution is shown by With et al. by measuring the concentration-induced lyotropic phase transition of PI-PEO polymers. Employing a simple cross-shaped multilayer Kapton microfluidic device (**Figure 3A-C**) in combination with synchrotron microfocus SAXS, time-resolved self-assembly of the used PI-PEO polymers via a spinodal microphase to micelles into FCC liquid-crystalline phases could be studied with millisecond resolution [40]. A more sophisticated channel design was used to study the self-assembly of PI-PEO block copolymers via spherical micelles into a FCC lattice (**Figure 3G-J**) and the solvent-induced self-assembly of PEG-PLAinto spherical micelles, cylindrical micelles and vesicles by Fürst et al. [23].

Apart from surfactants, polymers and polymer coated particles, other materials have self-assembly properties and can be investigated with a combination of microfluidics and X-ray scattering. Seibt et al. followed the pH-induced, rapid assembly of disk-shaped hydrogelators (N,N′,N″-tris(4-carboxyphenylene)-1,3,5-benzene tricarboxxamide) to nanofibrils of several hundred nanometres length by CLSM and SAXS. The measurement of the self-assembly process utilised 3D hydro-dynamic focusing microfluidic devices (**Figure 3D-F**). Even bigger structures could be followed in the case of collagen and collagen derived fibres by pH-induced self-assembly. Here microfluidic chips provide an excellent platform for wet-spinning processes, shown by Haynl et al. [44] and Hofmann et al. [45], while SAXS can provide important information about the internal structure of the fibres during formation [46]. Furthermore, the alignment of macromolecular structures, such as worm-like micelles, patchy polymers and nanoplatelets can be investigated in (tapering) channels *on chip* [47] as well as in free jets (**Figure 3K-M**) [48].
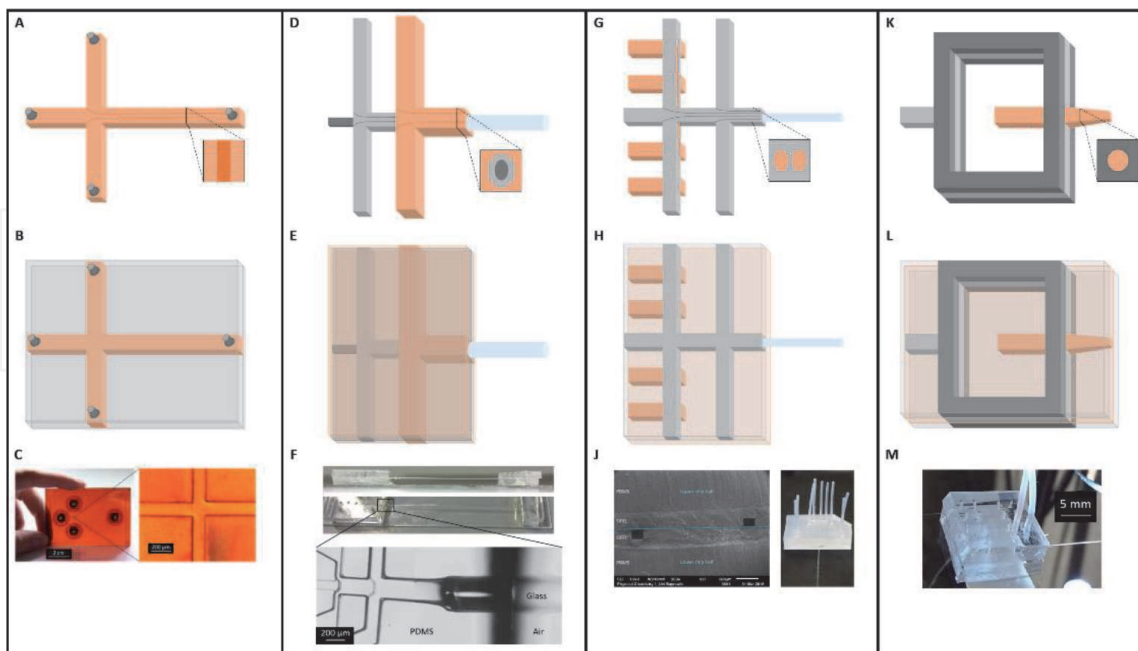

Figure 3.
Schematics and images of microfluidic devices used for time-resolved nanoparticle nucleation and growth and macromolecular self-assembly. (A) T-shaped, single layer (B) hydrodynamic focusing microfluidic device, made from Kapton (C) [40]. (D) Three-dimensional (multilayer) hybrid hydrodynamic focusing device (E), made from PDMS with inserted glass capillary (F) [24]. (G) Double stream hydrodynamic focusing device, which can be aligned without optical access (H), made from SIFEL with a thin PDMS carrier layer and inserted glass capillary (J) [23]. (K) Multilayer (L) micro-jet device with hydrodynamic focused spray out of a nozzle, made entirely from PDMS (M) [41].

4. Conclusion and outlook

Many hypotheses posed by researchers across the world would be answered by observing reactions in real time. To achieve this, two major technologies provide significant opportunity when merged: SAXS and optimised microfluidic setups. Although the last decades of research lead to significant developments in combining these fields, it remains a demanding intersection of methods with the potential to answer many fundamental questions around nucleation, growth and self-assembly of materials on the nanoscale. New three-dimensional hydrodynamic focusing device designs show great promise in studying a variety of systems – from organic to inorganic and crystal growth to self-assembly processes. Nevertheless, this is still an emerging field, with microfluidic and synchrotron technologies continuing to push the boundaries of possible experiments, opening up new possibilities for further reducing dead times, and thereby understanding the earliest parts of synthesis reactions, which are of critical importance in future control and modification of nanoparticles for a wide variety of purposes. Micro-focused X-ray beams and beamline optimisation, meanwhile, will be a key component to access faster timescales with SAXS. We hope that this overview of microfluidics and SAXS analyses, along with some of our insights will aid future investigations into this challenging, but exciting field.

Acknowledgements

Conflict of interest

The chapter was written through contributions of all authors. All authors have given approval of the version of the chapter. The authors declare no competing financial interest.

Author details

Susanne Seibt* and Timothy Ryan
Australian Synchrotron, ANSTO, Melbourne, Victoria, Australia

*Address all correspondence to: seibts@ansto.gov.au

IntechOpen

References

[1] Manz A, Graber N, Widmer HM. Miniaturized total chemical analysis systems: A novel concept for chemical sensing. Sensors and Actuators B: Chemical. 1990;1:244–8.

[2] Kopp MU, Mello AJ, Manz A. Chemical amplification: continuous-flow PCR on a chip. Science. 1998;280: 1046–8.

[3] Harrison DJ, Fluri K, Seiler K, Fan Z, Effenhauser CS, Manz A. Micromachining a miniaturized capillary electrophoresis-based chemical analysis system on a chip. Science. 1993; 261:895–7.

[4] Hadd AG, Raymond DE, Halliwell JW, Jacobson SC, Ramsey JM. Microchip device for performing enzyme assays. Anal Chem. 1997;69:3407–12.

[5] Woolley AT, Mathies RA. Ultra-high-speed DNA sequencing using capillary electrophoresis chips. Anal Chem. 1995; 67:3676–80.

[6] Manz A, Harrison DJ, Verpoorte EMJ, Fettinger JC, Paulus A, Lüdi H, et al. Planar chips technology for miniaturization and integration of separation techniques into monitoring systems. Journal of Chromatography A. 1992;593:253–8.

[7] Ingham B. X-ray scattering characterisation of nanoparticles. Crystallography Reviews. 2015;21:229– 303.

[8] Squires TM, Quake SR. Microfluidics: Fluid physics at the nanoliter scale. Reviews of Modern Physics. 2005;77: 977–1026.

[9] Neto C, Evans DR, Bonaccurso E, Butt H-J, Craig VSJ. Boundary slip in Newtonian liquids: a review of experimental studies. Reports on Progress in Physics. 2005;68:2859–97.

[10] Lee CY, Chang CL, Wang YN, Fu LM. Microfluidic mixing: a review. Int J Mol Sci. 2011;12:3263–87.

[11] Ward K, Fan ZH. Mixing in microfluidic devices and enhancement methods. J Micromech Microeng. 2015;25.

[12] Capretto LC, W; Hill, M; Zhang,X. Micromixing Within Microfluidic Devices. Microfluidics. Berlin, Heidelberg: Springer; 2011. p. 27–68.

[13] Feigin LA, Svergun DI, Taylor GW. Structure Analysis by Small-Angle X-Ray and Neutron Scattering. Boston, MA: Springer US; 1987.

[14] Bruus H. Theoretical microfluidics. Oxford: Oxford University Press; 2008.

[15] Lu M, Ozcelik A, Grigsby CL, Zhao Y, Guo F, Leong KW, et al. Microfluidic Hydrodynamic Focusing for Synthesis of Nanomaterials. Nano Today. 2016;11:778–92.

[16] McDonald JC, Duffy DC, Anderson JR, Chiu DT, Wu H, Schueller OJA, et al. Fabrication of microfluidic systems in poly (dimethylsiloxane). Electrophoresis. 2000;21:27–40.

[17] Duffy DC, McDonald JC, Schueller OJ, Whitesides GM. Rapid Prototyping of Microfluidic Systems in Poly(dimethylsiloxane). Anal Chem. 1998;70:4974–84.

[18] Xia Y, Whitesides GM. Soft Lithography. Angewandte Chemie International Edition. 1998;37: 550–75.

[19] Heckele M, Bacher W, Müller KD. Hot embossing - The molding technique for plastic microstructures. Microsystem Technologies. 1998;4:122–4.

[20] Becker H, Heim U. Hot embossing as a method for the fabrication of polymer high aspect ratio structures. Sensors and Actuators A: Physical. 2000;83:130–5.

[21] Amin R, Knowlton S, Hart A, Yenilmez B, Ghaderinezhad F, Katebifar S, et al. 3D-printed microfluidic devices. Biofabrication. 2016;8:022001.

[22] Bishop GW. 3D Printed Microfluidic Devices. Microfluidics for Biologists: Springer; 2016. p. 103–13.

[23] Fuerst C. Kinetic studies of lyotropuc structure formation with microfluidics and small angle X-ray scattering [Dissertation]. Bayreuth: University of Bayreuth; 2016.

[24] Seibt S, Mulvaney P, Förster S. Millisecond CdS nanocrystal nucleation and growth studied by microfluidics with in situ spectroscopy. Colloids and Surfaces A: Physicochemical and Engineering Aspects. 2019;562:263–9.

[25] Seibt S. In-situ Investigations of Molecular Self-Assembly Using Microfluidics [Dissertation]. Bayreuth, Melbourne: University of Bayreuth, The University of Melbourne; 2018.

[26] Chen X, Schroder J, Hauschild S, Rosenfeldt S, Dulle M, Forster S. Simultaneous SAXS/WAXS/UV-Vis Study of the Nucleation and Growth of Nanoparticles: A Test of Classical Nucleation Theory. Langmuir. 2015;31: 11678–91.

[27] Herbst M, Hofmann E, Forster S. Nucleation and Growth Kinetics of ZnO Nanoparticles Studied by in Situ Microfluidic SAXS/WAXS/UV-Vis Experiments. Langmuir. 2019;35: 11702–9.

[28] Polte J, Ahner TT, Delissen F, Sokolov S, Emmerling F, Thunemann AF, et al. Mechanism of gold nanoparticle formation in the classical citrate synthesis method derived from coupled in situ XANES and SAXS evaluation. J Am Chem Soc. 2010;132:1296–301.

[29] Harada M, Tamura N, Takenaka M. Nucleation and Growth of Metal Nanoparticles during Photoreduction Using In Situ Time-Resolved SAXS Analysis. The Journal of Physical Chemistry C. 2011;115:14081–92.

[30] Henkel A, Schubert O, Plech A, Sönnichsen C. Growth Kinetic of a Rod-Shaped Metal Nanocrystal. The Journal of Physical Chemistry C. 2009;113: 10390–4.

[31] Garcia PRAF, Prymak O, Grasmik V, Pappert K, Wlysses W, Otubo L, et al. An in situ SAXS investigation of the formation of silver nanoparticles and bimetallic silver–gold nanoparticles in controlled wet-chemical reduction synthesis. Nanoscale Advances. 2020;2:225–38.

[32] Abecassis B, Testard F, Spalla O, Barboux P. Probing in situ the nucleation and growth of gold nanoparticles by small-angle X-ray scattering. Nano Lett. 2007;7:1723–7.

[33] Abecassis B, Testard F, Kong Q, Francois B, Spalla O. Influence of monomer feeding on a fast gold nanoparticles synthesis: time-resolved XANES and SAXS experiments. Langmuir. 2010;26:13847–54.

[34] Polte J. Fundamental growth principles of colloidal metal nanoparticles – a new perspective. CrystEngComm. 2015;17:6809–30.

[35] Polte J, Erler R, Thunemann AF, Sokolov S, Ahner TT, Rademann K, et al. Nucleation and growth of gold nanoparticles studied via in situ small angle X-ray scattering at millisecond time resolution. ACS Nano. 2010;4: 1076–82.

[36] Polte J, Erler R, Thunemann AF, Emmerling F, Kraehnert R. SAXS in combination with a free liquid jet for improved time-resolved in situ studies of the nucleation and growth of nanoparticles. Chem Commun (Camb). 2010;46:9209–11.

[37] Gerstner D, Kraus T. Rapid nanoparticle self-assembly at elevated temperatures. Nanoscale. 2018;10: 8009–13.

[38] Merkens S, Vakili M, Sanchez-Iglesias A, Litti L, Gao Y, Gwozdz PV, et al. Time-Resolved Analysis of the Structural Dynamics of Assembling Gold Nanoparticles. ACS Nano. 2019;13: 6596–604.

[39] Nette J, Howes PD, deMello AJ. Microfluidic Synthesis of Luminescent and Plasmonic Nanoparticles: Fast, Efficient, and Data-Rich. Advanced Materials Technologies. 2020;5.

[40] With S, Trebbin M, Bartz CB, Neuber C, Dulle M, Yu S, et al. Fast diffusion-limited lyotropic phase transitions studied in situ using continuous flow microfluidics/ microfocus-SAXS. Langmuir. 2014;30: 12494–502.

[41] Trebbin M, Kruger K, DePonte D, Roth SV, Chapman HN, Forster S. Microfluidic liquid jet system with compatibility for atmospheric and high-vacuum conditions. Lab Chip. 2014;14: 1733–45.

[42] Schiener A, Wlochowitz T, Gerth S, Unruh T, Rempel A, Amenitsch H, et al. Nucleation and growth of CdS nanoparticles observed by ultrafast SAXS. MRS Proceedings. 2013;1528.

[43] Stegelmeier C, Exner A, Hauschild S, Filiz V, Perlich J, Roth SV, et al. Evaporation-Induced Block Copolymer Self-Assembly into Membranes Studied by in Situ Synchrotron SAXS. Macromolecules. 2015;48:1524–30.

[44] Haynl C, Hofmann E, Pawar K, Forster S, Scheibel T. Microfluidics-Produced Collagen Fibers Show Extraordinary Mechanical Properties. Nano Lett. 2016;16:5917–22.

[45] Hofmann E, Kruger K, Haynl C, Scheibel T, Trebbin M, Forster S. Microfluidic nozzle device for ultrafine fiber solution blow spinning with precise diameter control. Lab Chip. 2018;18:2225–34.

[46] Dehsorkhi A, Castelletto V, Hamley IW, Adamcik J, Mezzenga R. The effect of pH on the self-assembly of a collagen derived peptide amphiphile. Soft Matter. 2013;9.

[47] Trebbin M, Steinhauser D, Perlich J, Buffet A, Roth SV, Zimmermann W, et al. Anisotropic particles align perpendicular to the flow direction in narrow microchannels. Proc Natl Acad Sci U S A. 2013;110:6706–11.

[48] Schlenk M, Hofmann E, Seibt S, Rosenfeldt S, Schrack L, Drechsler M, et al. Parallel and Perpendicular Alignment of Anisotropic Particles in Free Liquid Microjets and Emerging Microdroplets. Langmuir. 2018;34: 4843–51.